

1 Advancement in fruit drying through the analysis of moisture sorption 2 isotherms: processing effects on Australian native fruits in comparison to apple

3 Paul Michalski^a, Md. Shahruk Nur-A-Tomal^a, Simon Crawford^b, Murray Rudman^c, Leonie van 't Hag^{a,*}

4 ^a Department of Chemical and Biological Engineering, Monash University, Clayton, VIC, 3800, Australia

5 ^b Ramaciotti Centre for Cryo-EM, Monash University, Clayton, VIC, 3800, Australia

6 ^c Department of Mechanical and Aerospace Engineering, Monash University, Clayton, VIC, 3800,
7 Australia

8 *Corresponding author. *E-mail address: leonie.vanthag@monash.edu*

9 Keywords

10 fruit, food drying, sustainable processing, moisture sorption, native foods, dynamic vapour sorption

11 Abstract

12 Australian native fruits are well-adapted to local climate and have growing interest in their nutritional
13 and sensory qualities. Among the most highly produced are finger limes and muntries. However,
14 published literature on their characterisation and especially their processing is limited. Water binding
15 in foods is linked to their preservation through the amount of water microbes need to be active and
16 the drying energy required. How processing affects this binding, however, is poorly understood. This
17 work studied the water binding of apples compared with muntries and finger limes. Unlike in apple,
18 water binding in native fruits was observed to increase after drying. This was correlated to increased
19 breakdown of complex carbohydrates into simple sugars in native fruits. It is suggested this may be a
20 feature of their drought adaptation. Together with a newly proposed equation for the drying heat
21 required, these findings can guide more sustainable processing of Australian native fruits.

22 1. Introduction

23 Fruits and vegetables are essential components of human diets, particularly due to their high
24 concentration of fibre and micronutrients. Their rapid spoilage and quality/nutritional degradation is
25 largely the result of their high moisture contents. The varying structure and chemistry of dry matter in
26 fruits determines their water binding capacity. Two foods of the same moisture content can have

27 substantial differences in the availability of that water for participation in degradation pathways, as
28 quantified by the water activity (Jeantet, 2016). Water activity plays an important role in a food's shelf-
29 stability, with correlations between the two being the subject of modelling. For example, Escobedo-
30 Avellaneda et al. (2012) modelled the shelf-life of packaged vegetables dried to different extents. They
31 found that knowing the water activities of these vegetables across a range of moisture contents,
32 together with packaging permeation and area, could be used to predict how the probability of spoilage
33 accumulated with time. The correlation between the water content and the water activity for a food
34 as determined by measuring moisture sorption isotherms can therefore be used to engineer the
35 processing conditions to improve shelf-life.

36 Isotherms for the sorption of water to the food matrix have for example been measured for apples,
37 bananas, pineapples, grapes, apricots, tomatoes, carrots, potatoes, loquat, quince, and kiwifruit
38 (Moraga et al., 2011, Kaymak-Ertekin and Gedik, 2004, Hossain et al., 2001, Kiranoudis et al., 1993,
39 Moreira et al., 2008, Moraga et al., 2006). A number of different models have been proposed and
40 tested as descriptors of these isotherms, including those suggested by Henderson, by Guggenheim,
41 Anderson and de Boer (GAB), and by Brunauer, Emmett and Teller (BET) (Al-Muhtaseb et al., 2002).
42 These have allowed for a more rigorous understanding of the interaction between foods and the water
43 they contain. For example, fitting the GAB model to sorption isotherms of freeze-dried banana and
44 apple at 20°C, Moraga et al. (2011) found a monolayer moisture content of 8.1% for the freeze-dried
45 banana and 8.6% for the freeze-dried apple (see Section 3). This is representative of the 4-22% range
46 typically reported for fruits and vegetables (Tsami et al., 1998, Kaymak-Ertekin and Gedik, 2004,
47 Moraga et al., 2006, Kiranoudis et al., 1993, van 't Hag et al., 2020). Measurement and modelling of
48 water sorption in a range of food materials has given insight into their water binding and shelf-stability.

49 Processing of fruits and vegetables affects water behaviour within them and therefore shelf-life. This
50 phenomenon is not as well described, with most isotherms existing for the fresh or freeze-dried
51 material only. However, in examples such as the work of Ben Haj Said et al. (2015) and van 't Hag et al.
52 (2020), processing was shown to have significant effects on the water sorption in apples and African
53 leafy vegetables. In the study of the effects that dehydration (via instant controlled pressured drop) as
54 a pretreatment to freezing had on apple, Ben Haj Said et al. measured the sorption characteristics of
55 this partially dried material before and after freezing. The consistent decrease measured in equilibrium
56 moisture content post-freezing was correlated to the effect both drying and freezing had on apple
57 drying and rehydration kinetics as well as changes in firmness. Pre-drying in this case was shown to
58 eliminate the softening that freeze-thawing had on texture. In research on African leafy vegetables by
59 van 't Hag et al., the effect of drying was investigated by measuring how sorption isotherms differed

60 before and after drying at 40°C. Here equilibrium moisture contents were lower across water activities
61 for all samples measured after drying. This was correlated to drying-induced losses of cell structure
62 observed using TEM. Correlating the changes in sorption isotherms with changes in micro- and
63 nanostructure, texture, and rehydration ability allowed these researchers to better understand the
64 changes that occurred during processing and so suggest best processing methods and conditions.

65 How food moisture sorption isotherms vary with temperature can elucidate the capacity and the
66 energy of the binding between water and the food matrix. For example, the BET-defined monolayer
67 moisture content, fitted to the sorption isotherms of grapes, apricots, apples, and potatoes, was shown
68 to decrease with temperature between 30°C and 60°C (Kaymak-Ertekin and Gedik, 2004). The
69 measurement of the temperature-dependence of sorption has also allowed the moisture content-
70 dependent heat required to liberate water from its binding to the matrix to be determined. The net
71 isosteric heat of sorption, or the heat required in excess of the latent heat of vaporisation to remove
72 moisture from the food, was reported for dried raisins, figs, prunes, and apricots (Tsami et al., 1990).
73 As moisture content decreased, the heat of sorption was observed to dramatically increase, which the
74 authors attributed to the sorption of a monolayer being preferred at low moisture contents. The net
75 isosteric heat of sorption and its dependence on moisture content was not observed to substantially
76 differ between these fruits. A model was used to fit the heat of sorption that was obtained for these
77 materials, but this was purely empirical.

78 Australian native fruits (ANFs) are among the tens of thousands of plant species unique to Australia
79 and have a long history of appreciation by First Nations Australians. Their evolution in Australian
80 climate and soil means they are inherently better adapted to these conditions than introduced crops,
81 frequently displaying a reduced need for irrigation, pesticide and fertiliser use, as well as an increased
82 tolerance to droughts, floods, and heatwaves (Orians and Milewski, 2007). These latter features
83 particularly make them crops of interest for ensuring future food security as climate change raises
84 temperatures and increases the threat of extreme weather events (Seneviratne et al., 2023). Finger
85 limes and muntries are among the most highly produced ANF crops. In 2019/2020 they were produced
86 at a rate of 103 and 3.4 tonnes/year respectively within Australia (Laurie, 2020). This industry is
87 growing, with the farm gate market value projected to grow by 8.0% p.a. for finger limes and 2.8% p.a.
88 for muntries between 2019/2020 and 2025. The market interest in ANFs is both within Australia as
89 well as overseas. For example, as of 2021, 10 tonnes/year of finger lime are exported internationally,
90 while global cultivation efforts have begun that include 12,000 trees in California and 100,000 trees in
91 Guatemala (Glover et al., 2021). ANFs have also been shown to contain high amounts of protein and
92 phenolic compounds (a class of antioxidants) compared to more commonly eaten fruits (Richmond et

93 al., 2019). However, nutritional and phytochemical characterisation of ANFs is still incomplete (Table
 94 1), and where values are available the data is limited and often from one batch grown in one location.

95 *Table 1: Selected data on previously reported nutritional data for ANFs where available (per 100 g w.b.). Data for apple is*
 96 *also presented for comparison (GAE: gallic acid equivalent, -: no published data found, G: glucose, S: sucrose, F: fructose, 1:*
 97 *(USDA, 2018), 2: (Netzel et al., 2007), 3: (Richmond et al., 2019), 4: (Francini and Sebastiani, 2013))*

	Apple	Muntrie	Finger Lime
Protein (g)	0.26 ¹	-	1.6 ³
Fat (g)	0.17 ¹	-	1.0 ³
Carbohydrate (g)	13.8 ¹	-	5 ³
Sugars (g)	2.43 ^G /2.07 ^S /5.9 ^{F,1}	-	1.2 ^{F+G,3}
Vitamin C (mg)	4.6 ¹	16 ²	58.5 ³
Total Phenolics (mmol GAE)	0.070-3.442 ⁴	6.712 ²	8.65-10.93 ²
Energy (kJ)	218 ¹	-	144-411 ³

98 While the industry of their cultivation and processing is growing, an understanding of how ANFs are
 99 affected by processing, specifically preservation, is absent from literature. For larger-scale process
 100 engineering of ANFs, a rigorous understanding of their processing-property relationships is needed.
 101 This would extend their shelf-lives and increase market penetration of ANFs while minimising quality
 102 loss and the cost and energy of processing. Through such an understanding of ANFs, the processing of
 103 more climate-tolerant crops in general, which may have different moisture sorption regulation
 104 properties, may be enabled to better protect future food security.

105 The research described in this work, therefore, characterises the moisture sorption phenomena in the
 106 ANFs muntries and finger limes as well as apples for comparison. This informs the minimum extent of
 107 drying that must be performed to achieve products with a range of water activities. How oven- and
 108 freeze-drying affected the sorption behaviour of these fruits, as well as qualities associated with water
 109 binding such as crystallinity, carbohydrate chemistry, and ultrastructure, were also examined. Changes
 110 in these latter properties were used to describe the processing-structure correlations that exist in
 111 apple, not previously reported in literature, as well as the measured ANFs. The measured sorption
 112 phenomena were modelled to describe facets of water binding dynamics. Based on these models a
 113 new analytical expression was derived that accurately approximates the energy requirements of
 114 drying. To the best of our knowledge, no analytical expression has been reported for the functional
 115 dependence of the net isosteric heat of sorption on moisture content for any food before. Such an
 116 expression has value in designing and optimising more bespoke dryers for the processing of ANFs as

117 well as other foods. These findings will inform the minimal but effective preservation of fruits and the
118 minimum energy required to be able to do this for more sustainable processing.

119 2. Materials and Methods

120 2.1. Materials

121 Analytical grade petroleum ether, propylene oxide, magnesium chloride (99.99% purity), potassium
122 chloride (99.8% purity), and lithium chloride (99.98% purity) were sourced from Merck Life Science
123 (Bayswater, Victoria, Australia). A Megazymes K-SUFRG Sucrose/D-Glucose/D-Fructose enzymatic
124 assay kit was obtained from Bio-Strategy (Campbelfield, Victoria, Australia), and 2,5-bis(5-tert-butyl-
125 2-benzo-oxazol-2-yl) thiophene (BBOT) from Thermo-Fisher Scientific (Scoresby, Victoria, Australia).
126 Pure (grade 4.2) compressed nitrogen was supplied by BOC (Dandenong South, Victoria, Australia) and
127 Epon/Araldite resin by Electron Microscopy Sciences (Hatfield, Pennsylvania, USA). Glutaraldehyde
128 (25%), paraformaldehyde (16%), uranyl acetate, lead citrate, potassium ferricyanide, sodium
129 cacodylate trihydrate, and osmium tetroxide were sourced from ProSciTech (Kirwan, Queensland,
130 Australia).

131 Muntries were donated by Ni Ni Well (Nhill, Victoria, Australia), finger limes (Rick's Red) were donated
132 by OZ Finger Lime (Glenroy, Victoria, Australia), and apples (Pink Lady) were purchased from Monash
133 Merchant (Clayton, Victoria, Australia). Whole fruits were air frozen at harvest (or after purchase in
134 the case of apple) at -18°C using a SFT45-2 freezer (Skipio, Campbelfield, Victoria) until analysed or
135 further processed. Freeze-drying of approximately 90 g of the frozen material was conducted at 0.04
136 mbar with an Alpha 1-2 LD-Plus freeze-dryer (John Morris, Victoria, Australia) until sample masses
137 changed by < 0.1 g/h. Oven-drying of the frozen material was conducted with a Memmert UF55 oven
138 (John Morris, Victoria, Australia). Approximately 90 g of fruit was dried at both 40°C and 60°C at 20%
139 fan speed and 50% vent opening until sample mass changed by < 0.1 g/h. Dried samples were
140 homogenised with a coffee grinder. They were then sealed using a FoodSaver® GameSaver™ VS9000
141 vacuum sealer (Sunbeam, NSW, Australia) in plastic vac-seal FoodSaver® pouches (Sunbeam, NSW,
142 Australia) for dry storage until analysis.

143 2.2. Methods

144 2.2.1. Dynamic Vapour Sorption (DVS)

145 Sorption and desorption isotherms were obtained by using a DVS Adventure 1 (Surface Measurement
146 Systems, London, UK). The instrument humidity control used an open control loop based on mass flow
147 controller calibration using saturated salt slurries of KCl, LiCl, and MgCl₂. Of the dried, packaged, and

148 stored samples described in Section 2.1, 17 mg of sample was loaded via a steel pan into the
149 instrument. The sample was allowed to equilibrate at 90% relative humidity, then 85%, 80%, 75%, 70%,
150 and then in decreasing steps of 10% until 0%, at which point it remained at 0% for 600 minutes before
151 increasing humidity in the reverse order. Equilibrium was considered reached once the sample mass
152 changed by less than 0.0012%/min of its mass at the beginning of each humidity step. The humid
153 atmosphere was generated through the supply of nitrogen and milliQ water to the instrument, and
154 the humid gas flow over the sample was 200 sccm (except at 60°C, where the flow was 100 sccm). For
155 dried samples, measurements were conducted two weeks after drying and dry storage at room
156 temperature.

157 2.2.2. XRD

158 The samples were placed on a PMMA sample holder (C79298A3244D82, Bruker, USA) featuring a
159 diameter of 51.5 mm and a height of 8.5 mm. X-ray diffraction patterns for the samples were obtained
160 using a D8 ADVANCE (Bruker, USA), utilising Cu-K α radiation at 40 kV and 40 mA. These patterns were
161 recorded over a 2θ range of 5° to 80°, with a step size of 0.010° and a step time of 144.0 s. The
162 DIFFRAC.EVA software package was used to determine the crystallinity and amorphous content of the
163 samples. First, the background of the patterns was set manually. Then, 'Compute Crystallinity' was
164 selected from the 'Crystallinity' tab, which provided values for Global Area and Reduced Area based
165 on the broad amorphous peak area.

166 2.2.3. TEM

167 Pieces of fruit tissue, approximately 1 mm³ in size, were placed into primary fixative for 24 hours at
168 room temperature. The fixative consisted of 2.5% glutaraldehyde and 2% paraformaldehyde in 0.1 M
169 sodium cacodylate buffer. The tissues were then rinsed twice in buffer for 1 hour. Secondary fixation
170 was performed using 1% osmium tetroxide and 1.5% potassium ferricyanide in cacodylate buffer for 2
171 hours at room temperature. The tissues were rinsed in three washes of milliQ water for 10 minutes
172 each and finally overnight in milliQ water.

173 The fixed tissues were dehydrated by incubating in increasing concentrations of ethanol for 24 hours
174 at each step, consisting of 30, 50, 70, 90 and 100% ethanol. Dehydrated tissues were incubated for 1
175 hour in 100% propylene oxide. Tissues were then incubated in a mixture of Epon resin and propylene
176 oxide at a ratio of 1:1 and 'biowaving' in a PELCO BioWave® Pro (Ted Pella Inc., California, USA) for 3
177 minutes at 250 W, followed by incubation for 24 hours at room temperature. This process of
178 'biowaving' and incubating for 24 hours was repeated with a 2:1 Epon/ethanol mixture and two steps

179 of 100% freshly made epon resin. Following the embedding steps the tissue samples were placed into
180 BEEM capsules with fresh resin and polymerised for 48 hours in an oven at 60°C.

181 Resin embedded tissue was sectioned with a Diatome diamond knife using a Leica UCS
182 ultramicrotome. Sections of thickness 80 - 90 nm were collected onto 150 mesh copper/palladium
183 grids and stained sequentially with 1% uranyl acetate for 10 minutes and lead citrate for 5 minutes.
184 The sections were imaged in a JEOL 1400+ transmission electron microscope (JEOL Ltd., Japan) at 80
185 kV, and images of cells captured with a digital camera at a resolution of 2K x 2K.

186 2.2.4. Macronutritional Profile

187 Freeze-dried samples were used for macronutrient characterisation. Moisture content was
188 determined in triplicate at 130°C using an MB25 moisture analyser (Ohaus, Victoria, Australia). Four
189 replicates of the protein content were measured through the CHNS combustion method, finding the
190 nitrogen content using a FlashSmart elemental analyser (Thermo-Fisher Scientific, Victoria, Australia)
191 and BBOT standards. A Kjeldahl factor of 5.36 was used to convert nitrogen content to protein content.
192 This was based on the work of Salo-väänänen and Koivistoinen (1996) which found more specific
193 Kjeldahl factors for different food groups as opposed to the value of 6.25 often used for food in general.

194 The standard AOAC method 2003.06 (AOAC, 2005) was the basis for the ash content measurements
195 (done in duplicate). Pre-weighed porcelain crucibles were loaded with samples and weighed before
196 being placed in a CF1200-4.5L muffle furnace (Across International, Victoria, Australia). Here the
197 sample crucibles were heated at 100°C for an hour before being heated at 525°C for 18 hours to dry
198 ash. After cooling, samples were inspected for evidence of charring. If present, a few drops of milliQ
199 water were added to the crucible before repeating the heating sequence until a pale grey fine ash
200 remained and could be weighed.

201 For the fat content, 4 g of sample was weighed into a cellulose thimble and subsequently placed in a
202 Soxhlet apparatus. Here 200 mL of petroleum ether was used to extract crude fat from the sample
203 over the course of 16 hours. The solvent was first evaporated from the extraction flask using a
204 Rotavapor R-210 rotary evaporator (In Vitro Technologies, Victoria, Australia) at 60°C and 580 mbar for
205 15 minutes. Residual solvent was then further dried in a 27G SEM drying oven (Labquip™, Victoria,
206 Australia) at 60°C until a consistent weight was measured. Fat contents were measured in duplicate.

207 Carbohydrate content was calculated by difference, i.e. the sample mass after subtraction of moisture,
208 protein, fat, and ash content. Energy content was calculated using the specific Atwater factors for fruit
209 of 14.1 kJ/g protein, 35 kJ/g fat, and 15.1 kJ/g carbohydrates (Merrill, 1973).

210 2.2.5. Sugar Contents

211 Sugar assays were performed on frozen samples (homogenised immediately prior to analysis) and
212 samples that had been oven-dried, each in triplicate. Samples were each added to 400 mL milliQ water
213 before being sonicated for 30 minutes in a Sonorex RK255/H/CH ultrasonic bath (John Morris, Victoria,
214 Australia). They then underwent syringe filtration using 0.45 µm Supor® membranes in 25 mm
215 Acrodisc® filters (Pall Corporation, New York, USA) and dilution in milliQ water by a factor of 3. These
216 solutions were then assayed according to the Megazymes K-SUFRG Sucrose/D-Glucose/D-Fructose
217 protocol. A Multipette® M4 - Multi-Dispenser pipette (Eppendorf, NSW, Australia) was used for the
218 dispensation of solutions for the assay. The assays were performed in 10 x 10 x 45 mm polystyrene
219 cuvettes (Sarstedt, Nümbrecht, Germany) and absorbances were measured at 340 nm using a Cary 60
220 UV-Vis Spectrophotometer (Agilent, Victoria, Australia).

221 3. Theory/Calculation

222 3.1. Moisture Sorption Isotherms

223 A number of models have been used in describing water sorption phenomena in foods. Ten common
224 models were selected as candidates for modelling ANF sorption. These were the Oswin, Brunauer-
225 Emmett-Teller (BET), Guggenheim-Anderson-de Boer (GAB), Halsey, Chen, Chung-Pfost, Henderson,
226 Caurie, Sips, and Iglesias-Chirife models (Kaymak-Ertekin and Gedik, 2004, van 't Hag et al., 2020).
227 Empirical, semi-empirical, and analytical models are included in this selection, and their definitions are
228 included in the Supplementary Information Appendix 2 Table S1.

229 The Oswin, Henderson, Chen, Chung-Pfost and Iglesias-Chirife models are empirical, with Iglesias-
230 Chirife also including a term $M_{0.5}$ for the moisture content at a water activity of 0.5 (Al-Muhtaseb et
231 al., 2002, Chung and Pfost, 1967, Iglesias and Chirife, 1978). The Sips model expresses heterogeneous
232 sorption with its constants K_S , N , and C describing the capacity, intensity, and energy of sorption
233 respectively. In contrast, the Halsey model describes sorption of multilayers spanning a larger distance
234 from the surface, with k being an empirical constant and n quantifying the decay in potential binding
235 energy as distance is increased. The BET and Caurie models also depict sorption as occurring in layers,
236 with a monolayer moisture content M_0 and a constant C related to the heat of sorption. The GAB model
237 describes sorption as the binding of a monolayer of the water adsorbate to the food surface, as well
238 as the binding of multilayers of adsorbate on top of this monolayer. These multilayers are energetically
239 distinct from the monolayer but themselves undifferentiated. Because the GAB model was found to

240 best fit the data in this work (see Section 4.1) it was used for the derivation of an analytical expression
 241 of the net isosteric heat of sorption as outlined in Section 3.2. The GAB model is expressed in Eq. (1).

$$M = \frac{M_0 K C a_w}{(1 - K a_w)(1 + (C - 1) K a_w)} \quad (1)$$

242 Eq. (1) gives a functional relationship between the water activity a_w and the moisture content (on a
 243 dry basis) M . The model includes the parameters M_0 (the monolayer moisture content), K (a
 244 thermodynamic quantity associated with multilayer sorption), and C (a thermodynamic quantity
 245 associated with monolayer sorption). The latter two parameters are also described by the model as
 246 having an Arrhenius-type temperature dependence in Eq. (2-3). Here, H_l is the enthalpy of the bulk
 247 adsorbate material, H_m is the enthalpy of the adsorbate in the monolayer, and H_n is the enthalpy of the
 248 adsorbate in the multilayers. Here and throughout this work, R and T are the universal gas constant
 249 and the absolute temperature. The pre-exponential factors K_0 and C_0 are temperature-independent
 250 entropic parameters associated again with the thermodynamics of multi- and monolayer sorption
 251 respectively.

$$K = K_0 e^{\frac{H_l - H_n}{RT}} \quad (2)$$

$$C = C_0 e^{\frac{H_n - H_m}{RT}} \quad (3)$$

252 3.2. Net Isosteric Heat of Sorption

253 If the bulk adsorbate material behaves as an ideal gas under the measurement conditions, the
 254 temperature-dependence of its latent heat of vaporisation is considered negligible, and its specific
 255 volume when adsorbed is insignificant compared to its bulk specific volume, the Clausius-Clapeyron
 256 equation can be expressed in terms of the net isosteric heat of sorption (q_{st}) as Eq. (4).

$$q_{st}(M) = R \left(\frac{\partial \ln(a_w)}{\partial \left(\frac{1}{T}\right)} \right)_M = Q_{st}(M) - \Delta H_v \quad (4)$$

257 In Eq. (4) Q_{st} is the isosteric heat of sorption and ΔH_v is the latent heat of vaporisation of the adsorbate
 258 material. Thus, q_{st} is a measure of the energy required in excess of the latent heat of vaporisation to
 259 liberate a unit amount of adsorbate to the bulk phase at a given moisture content.

260 Limited empirical approaches and no analytical approaches have been reported to model the
 261 functional dependence of q_{st} on the moisture content. Since the GAB isotherm model is analytical and
 262 best fit the measured isotherms (Section 4.1), it was used to derive an analytical expression for q_{st} .
 263 Expressing the GAB model in terms of M yields Eq. (5).

$$a_w = \frac{\zeta + \sqrt{\zeta^2 - 4M^2(1-C)}}{2MK(C-1)} \quad (5)$$

Where $\zeta \equiv M(C-2) - M_0C$

264 Solving Eq. (4) using Eq. (5) yields, after simplification (see Supplementary Information Appendix 3 for
 265 detailed derivation) Eq. (6).

$$q_{st}(M) = R \frac{\left(\psi + \frac{\zeta\psi + 2M^2 \frac{H_n - H_m}{R}}{\sqrt{\zeta^2 - 4M^2(1-C)}} \right) C(C-1) - \left(\frac{H_l - H_n}{R} (C-1) + \frac{H_n - H_m}{R} C \right) (\zeta + \sqrt{\zeta^2 - 4M^2(1-C)})}{(\zeta + \sqrt{\zeta^2 - 4M^2(1-C)})(C-1)} \quad (6)$$

Where

$$\psi \equiv M \frac{H_n - H_m}{R} - \frac{dM_0}{d\left(\frac{1}{T}\right)} - M_0 \frac{H_n - H_m}{R}$$

266 Eq. (6) is an analytical model for the net isosteric heat of sorption with only five fitting parameters
 267 based on the sorption mechanisms described by the GAB model. It is expressed as a function of the
 268 moisture content and parametrised by the material-specific values of H_m , H_n , M_0 (and its derivative
 269 with respect to reciprocal temperature), and C . The parameter K is notably absent from the expression.
 270 The material-specific parameter associated with the entropy of multilayer sorption, K_0 , does not affect
 271 the net isosteric heat of sorption; the only influence of multilayer sorption is through the multilayer
 272 enthalpy H_n . The parameter C is assumed to follow an Arrhenius-type temperature dependence as
 273 described by Eq. (3). However, since the net isosteric heat of sorption is only weakly temperature-
 274 dependent at these scales, C represents a temperature-independent limit for the temperatures

275 considered. The value of M_0 as obtained by the fitting of Eq. (6) is taken as a temperature-independent
276 limit for the same reason, however it is not assumed to follow an Arrhenius-type relationship.

277 3.3. Statistical Analysis

278 Analysis was performed in MATLAB R2022a and used Eq. (7) and (8) for the goodness of fit (ν being
279 the number of degrees of freedom), including the sum of square errors (SSE). For access to the MATLAB
280 scripts written for this analysis, see Appendix 2.

$$SSE = \sum (y_i^{measured} - y_i^{predicted})^2 \quad (7)$$

$$\chi^2_\nu = \sum \frac{(y_i^{measured} - y_i^{predicted})^2}{\nu |y_i^{predicted}|} \quad (8)$$

281 Goodness of fit statistics are given for fits of the moisture sorption isotherms and net isosteric heats
282 of sorption (Table 2 and Supplementary Information Appendix 2 Tables S1 and S2). Differences in
283 protein values between fruits were analysed by a one-way ANOVA. The differences in sugar contents
284 between fruits and the differences before and after drying were analysed by a two-way ANOVA
285 followed by Tukey *post hoc* comparisons of the significantly different results.

286 4. Results and Discussion

287 The moisture sorption results of the DVS measurements are presented below, proceeded by the fitting
288 of the net isosteric heat of sorption derived from these measurements. Following this, the changes in
289 carbohydrate structure as measured by XRD and the changes in cellular structure as measured by TEM
290 are given. The macronutritional profiles and the changes to sugar composition are then described.
291 Finally, the changes to carbohydrate structure, cellular structure, and sugar composition are then
292 compared to the differences in the moisture sorption behaviour.

293 4.1. Moisture Sorption Isotherms

294 Moisture sorption isotherms as measured with DVS describe the binding of water to the food material
295 and relate how shelf-stability varies with moisture content. The changes in sample mass (and therefore
296 moisture content) were measured in response to changes in surrounding humidity. The relationship
297 between equilibrium moisture content and water activity for each measurement temperature formed

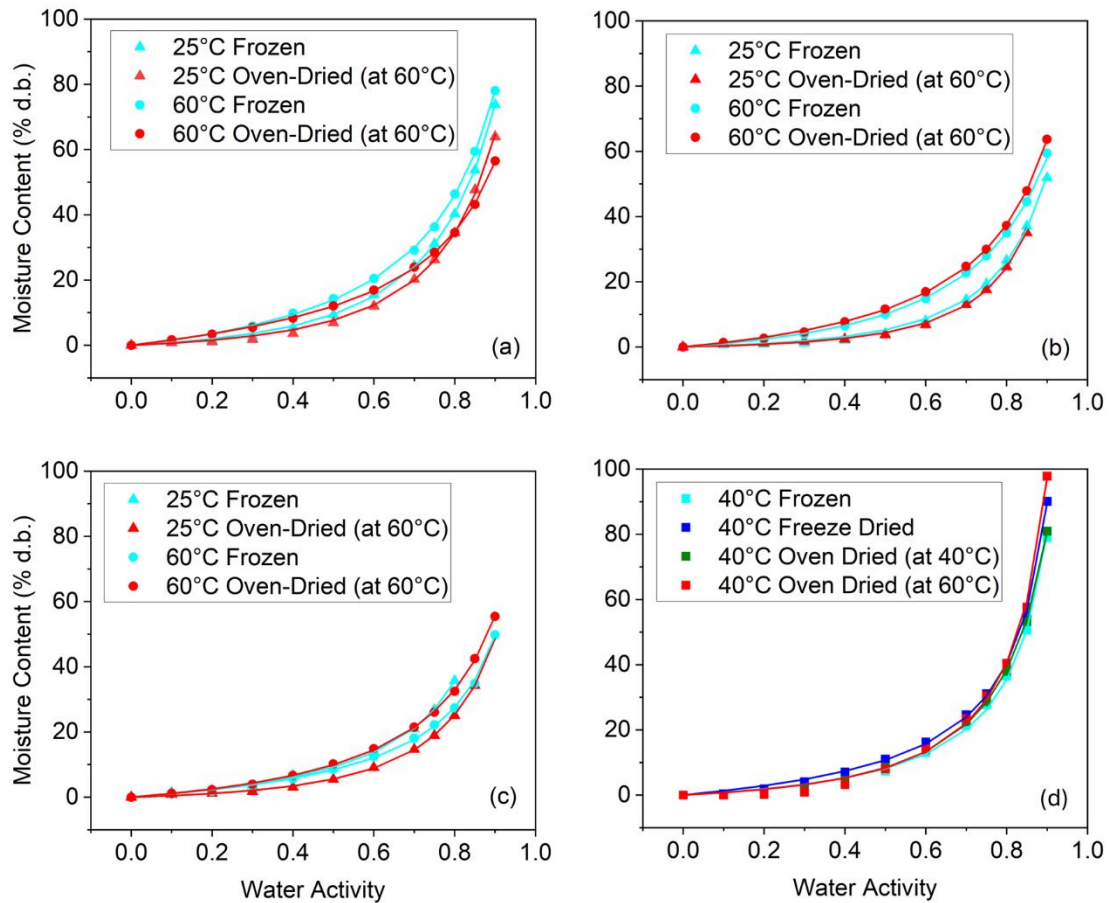
298 the moisture sorption isotherms. Isotherms measured at 25°C and 60°C for frozen and oven-dried (at
299 60°C) fruit samples are shown in Figure 1(a-c). Apples, muntries and finger limes all exhibited
300 significant increases in moisture content at high water activity, and relatively little change in moisture
301 content at lower water activity.

302 The shape and values taken by the isotherms are related to the class of food and its shelf-stability. The
303 observed isotherm shape is that of type-III isotherms, characteristic of high-sugar foods as previously
304 reported (Al-Muhtaseb et al., 2002, Rao et al., 2005). With minimal pathogenic proliferation at water
305 activities below 0.6, the moisture content to which this water activity corresponds is considered the
306 maximum microbially safe moisture content. From the desorption of frozen fruit (25°C isotherms), the
307 microbially safe moisture contents can be reported as 14% d.b. for finger lime, 8.0% for muntrie, and
308 15% for apple. In comparison, equivalent microbially safe moisture contents (interpolating water
309 activities and approximating with 30°C isotherms) measured by Kaymak-Ertekin and Gedik (2004) were
310 30% for grapes and 36% for apples. The moisture content measured in this work was lower in
311 comparison. In the work of Kaymak-Ertekin and Gedik (2004), however, the apple was frozen, and
312 freezing is seen to reduce the sorption that occurred in ANFs compared to select isotherms of fresh
313 fruit in Appendix 1 Figure S1. This is suggested to be the reason for the difference in microbially safe
314 moisture content of apple. This is also consistent with the effect of freezing on sorption described in
315 the work of Ben Haj Said et al. (2015) in Section 1.

316 Isotherms at 25°C showed that oven-drying (at 60°C) frozen fruit consistently reduced the equilibrium
317 moisture content for all water activities. In contrast, isotherms measured at 60°C showed that, for
318 muntrie and finger lime, oven-drying (at 60°C) increased the equilibrium moisture contents for all
319 water activities compared to the frozen sample. This was the opposite for apple, where oven-drying
320 (at 60°C) reduced moisture sorption.

321 The effect was investigated further for 40°C isotherms and included muntries that had been oven-dried
322 (at 40°C) and freeze-dried (Figure 1(d)). At this measurement temperature, freeze-dried muntries
323 bound more water than the oven-dried (at 40°C), which in turn bound more water than the frozen
324 muntries at all water activities. The oven-dried (at 60°C) muntries bound the most water for water
325 activities greater than 0.75 among the 40°C isotherms. It was also this water activity window of 0.60 -
326 0.75 in which the effects of isotherm measurement temperature changed; below this water activity,
327 sorption uniformly increased with temperature, but for greater water activities the 40°C isotherms
328 showed greater equilibrium moisture contents. All drying processes increased the equilibrium

329 moisture content achieved at all measured water activities when measuring at 40°C. Additional
 330 isotherms generated are included in Supplementary Information Appendix 1 Figure S1.



331

332 *Figure 1: Select desorption isotherms (and best GAB fits) measured at 25°C and 60°C of frozen and oven-dried (dried at*
 333 *60°C): (a) apple; (b) muntie; (c) finger lime, as well as the 40°C isotherms describing the sorption of frozen munties (d)*
 334 *after a range of processing conditions: data (▪) and GAB fit (—)*

335 The increases in sorption observed in ANFs is contrary to what was measured for African leafy
 336 vegetables (van 't Hag et al., 2020), where sorption uniformly decreased after drying. It is also contrary
 337 to the wider observations of the irreversible changes fruits undergo during drying. These changes do
 338 not allow rehydration to the same extent as they could before drying when equilibrated to the same
 339 water activity (Ben Haj Said et al., 2015), let alone accumulate a greater moisture content. In this
 340 regards munties and finger lime display distinctly different sorption behaviour.

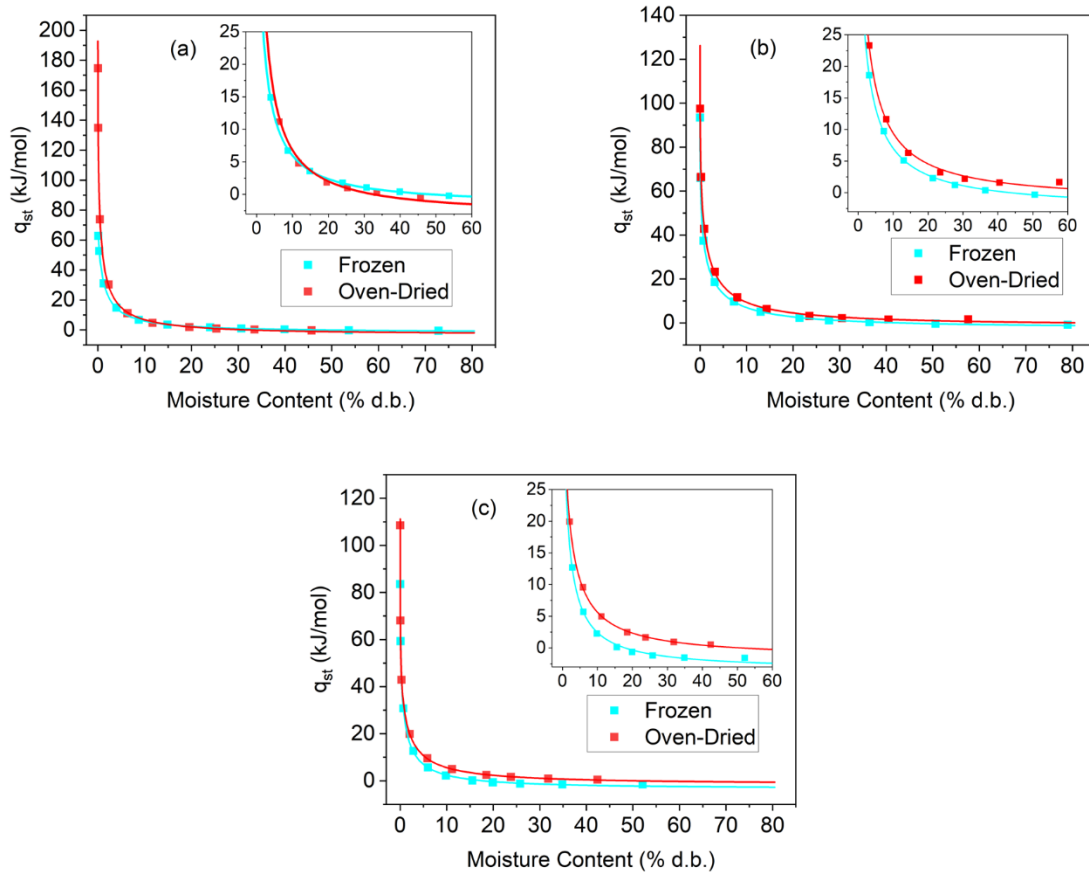
341 The performance of the models used to describe the sorption behaviour of these samples and the
 342 parameter values corresponding to their best fits are indicated in Supplementary Information
 343 (Appendix 2 Table S1) for the 60°C isotherm of frozen munties as a representative example. Since the

344 GAB model was consistently the isotherm model that minimised the SSE, it was selected as the most
345 accurate representation of the sorption mechanism in these systems. This being the case for individual
346 isotherms, isotherms for each sample were then fitted again. This time the isotherms corresponding
347 to a sample across the measured temperatures were fitted simultaneously to also fit the Arrhenius-
348 type temperature dependence of the model's parameters (Appendix 2 Table S2). By this latter fitting,
349 M_0 (which was allowed to vary with temperature) was found to take values between 7.1% d.b. in the
350 case of frozen muntries at 25°C and 25% in the case of oven-dried muntries at 60°C. These GAB
351 monolayer moisture contents were consistent with the ranges reported for other, relatively sugar-rich
352 fruits and vegetables as described in Section 1. To extend this model and improve the goodness of fit,
353 however, the net isosteric heat of sorption was modelled and presented in Section 4.2.

354 4.2. Net Isosteric Heat of Sorption

355 To transform the isotherm data collected into measured values of the net isosteric heat of sorption,
356 isosteres (curves following the relationship between a_w and T at constant M) were constructed for
357 muntries and finger limes using the moisture contents of the 40°C isotherms and interpolating the
358 25°C and 60°C isotherms to obtain the values of a_w at those moisture contents. For apple – without
359 data taken at 40°C – the moisture contents of the 25°C isotherms were used and the 60°C isotherms
360 were interpolated to find the values of a_w at those moisture contents. Transforming this data to show
361 how $\ln(a_w)$ varies with $1/T$, and assuming a negligible temperature-dependence of the net isosteric
362 heat of sorption, the gradient of the linear fit to each of these isosteres yields q_{st} for that value of M .

363 The net isosteric heat of sorption was then derived through the transformation of the isotherm data
364 as outlined in Section 3.2. The transformed data was then used to validate whether the newly
365 proposed model for q_{st} provided in Eq. (6) was valid. These experimentally derived values for $q_{st}(M)$, as
366 well as the best fit of the model described in Eq. (6) to these data, are shown in Figure 2.



367

368 *Figure 2: Net isosteric heat of sorption data (▪) and fitted models (–) of frozen and oven-dried (dried at 60°C): (a) apple; (b)*
 369 *muntrie; (c) finger lime. Inserts show moisture contents of 0 to 60% d.b. in the region of 0 to 25 kJ/mol to clarify differences*
 370 *and demonstrate the goodness of fit.*

371 The values of q_{st} were highest as moisture contents approached zero, sharply decreasing as moisture
 372 content increased. The functional shape exhibited by $q_{st}(M)$ is as expected for a high-moisture food.
 373 As described in Section 1, the amount of energy required to liberate water increases significantly as
 374 more water is removed (Tsami, 1991). This trend as well as the range of values adopted was consistent
 375 with those reported by Kaymak-Ertekin and Gedik (2004) for apple. The smoother curve of this new
 376 data is hypothesised to be due to the increased precision afforded by DVS compared to the static-
 377 gravimetric method. Compared to those reported by Kaymak-Ertekin and Gedik (2004), the generally
 378 reduced values of q_{st} here measured for apple are thought to be due to the effect of freezing in this
 379 study, which as identified in Ben Haj Said et al. (2015), can cause reduced sorption. To verify this, select
 380 isotherms of fresh ANF samples were also measured and supported the reduced sorption that occurs
 381 with freezing (Appendix 1 Figure S1). Bulk water with minimal binding is removed preferentially, then
 382 water in progressively more active sites is removed, requiring greater energy. Figure 2(b-c) shows that
 383 oven-drying affects muntries and finger limes in such a way as to increase the energy required for

384 moisture to escape at all moisture contents. For apple, on the other hand, this trend holds only where
385 $M < 0.15$, above which the trend reverses (Figure 2(a)). This is consistent with the isotherm results that
386 show increased water binding after drying in the case of the ANFs and not in the case of apple. This
387 phenomenon has not previously been reported for either conventional or native fruits. It is suggested
388 that the difference in this binding energy trend is associated with the increased water binding observed
389 in the isotherms of dried ANFs compared to frozen.

390 Fitting of the q_{st} data to the GAB-derived model (Eq. (6)) exhibits close agreement, quantified by the
391 SSE values listed in Table 2. The values obtained for C varied between 0.17 for oven-dried finger lime
392 and 0.32 for oven-dried apple. This range is consistent with the values for C obtained in literature by
393 isotherm modelling, e.g. the range of 0.42 - 1.54 obtained for sultanas by Maroulis et al. (1988). In
394 muntries and finger limes, the difference between the multilayer and bulk water enthalpy was
395 decreased from 2.71 to 1.58 and from 3.55 to 1.68 kJ/mol respectively by drying. In apple, drying
396 increased this difference from 1.78 to 3.40 kJ/mol. These enthalpy differences were similar in range to
397 those determined from the sorption isotherms of fresh apples (0.48 kJ/mol) and potatoes (3.49 kJ/mol)
398 by Kaymak-Ertekin and Gedik (2004). While drying raised the multilayer enthalpy in the ANFs, the
399 enthalpy difference between the mono- and multilayer increased more substantially with drying, from
400 298 to 359 kJ/mol in muntries and from 288 to 487 kJ/mol in finger lime. Once again following an
401 opposite trend, the corresponding change to the same enthalpy difference in apple decreased from
402 586 to 452 kJ/mol. Thus, while drying muntries and finger limes raises the enthalpy of the multilayer
403 to be closer to that of liquid water and decreases the enthalpy of the monolayer, the opposite occurs
404 as apples are dried. These enthalpy differences were an order of magnitude greater than the range of
405 values typically determined through isotherm modelling. For example, 23.4 kJ/mol was the average
406 value for this difference in enthalpy determined by Maroulis et al. (1988) for dried figs, prunes,
407 apricots, and raisins. Also, the monolayer moisture content was determined to have values between
408 0.14% and 0.31% d.b., approximately 2 orders of magnitude less than the monolayer moisture content
409 range literature provides for GAB fits to the isotherms as discussed in Sections 1 and 4.1. These
410 differences may arise from the combination of data at all temperatures to express a temperature-
411 independent net isosteric heat of sorption. For instance, the rate of change of monolayer moisture
412 content with respect to reciprocal temperature was determined to be about -100 K, i.e. the monolayer
413 moisture content strongly increases with temperature. The single value of M_0 determined here may
414 then be a low-temperature limit to the monolayer moisture content. More generally, it is suggested
415 the differences in values obtained by fitting the isotherms directly versus fitting the net isosteric heat
416 of sorption come from the temperature-independence of the latter.

417 Table 2: Values of net isosteric heat of sorption fitting parameters based on the sorption isotherms of frozen and oven-dried
 418 (at 60°C) apple, muntrie, and finger lime. Variation in fitting parameters is based on 68% confidence intervals. Extreme
 419 values which change the sign of the parameter are not considered physically meaningful.

	Apple		Muntrie		Finger Lime	
	Frozen	Oven-Dried	Frozen	Oven-Dried	Frozen	Oven-Dried
$C (-)$	0.2335 ±	0.3155 ±	0.2451 ±	0.2557 ±	0.2633 ±	0.1661 ±
	1.813	0.0192	0.0086	0.0992	0.0451	0.0026
M_0 (% d.b.)	0.138 ±	0.177 ±	0.309 ±	0.285 ±	0.175 ±	0.148 ±
	1.21	0.033	0.032	0.180	0.055	0.008
$H_n - H_m$ (kJ/mol)	585.5 ±	451.9 ±	298.1 ±	359.0 ±	288.3 ±	487.4 ±
	5841	74.23	24.63	251.35	102.3	15.311
$H_l - H_n$ (kJ/mol)	1.784 ±	3.399 ±	2.714 ±	1.581 ±	3.546 ±	1.677 ±
	0.155	0.4818	0.1684	0.55	0.3128	0.1239
$dM_0/d(1/T)$ (10 ³ K)	-0.1078 ±	-0.1389 ±	-0.1521 ±	-0.1676 ±	-0.0833 ±	-0.1078 ±
	0.0043	0.0084	0.0055	0.0173	0.0065	0.0027
SSE	0.2754	2.0682	0.2512	1.6421	0.9643	0.0989
χ_v^2	0.0066	0.3827	0.0424	0.1436	0.2618	0.0174

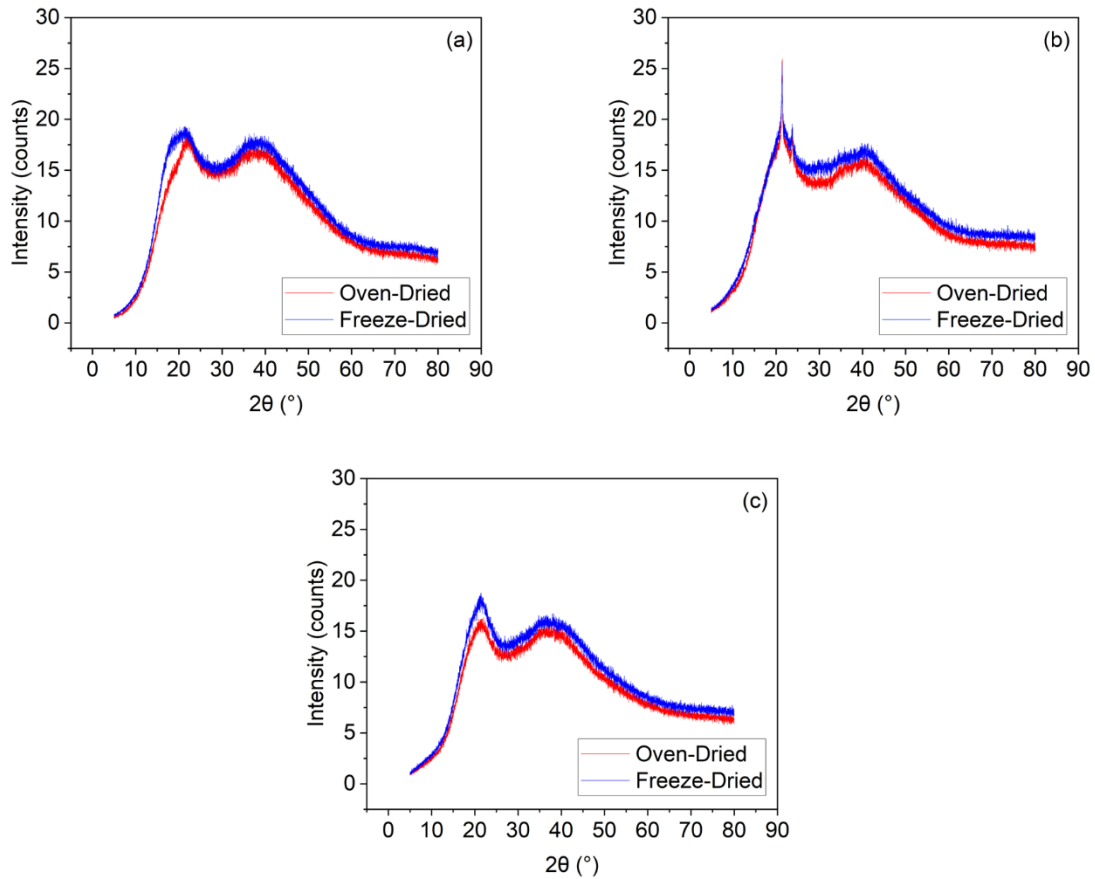
420 The goodness of fit for this proposed model, as quantified by χ_v^2 , takes into account the differences in
 421 both the degrees of freedom and the quantity being measured between these fits and those of
 422 Appendix 2 Table S2. This goodness of fit is better in the global fitting of the net isosteric heat of
 423 sorption than in the global fitting of the GAB isotherms at multiple temperatures for the majority of
 424 samples. One fewer parameter is also required with this approach due to the absence of a K term.
 425 Therefore, while the fitting to the net isosteric heat of sorption places additional assumptions as
 426 outlined above, the values of Table 2 (from the net isosteric heat of sorption) are those accepted here.
 427 The performance of this model supports the validity of the GAB model description of sorption, and
 428 with its validity thus supported this approach offers a new tool for food process engineering. The net
 429 isosteric heat of sorption q_{st} can be understood to be a differential quantity of heat required to liberate
 430 a differential quantity of water, changing the moisture content only infinitesimally. It is proposed then
 431 that the total heat per unit mass (dry basis) required to dry a food from an initial moisture content M_i
 432 to a desired final moisture content of M_f (which can be chosen using the sorption isotherms together
 433 with a choice of a_w and therefore shelf-life) can be predicted using Eq. (9).

$$Q_{M_i}^{M_f} = \frac{1}{MW} \left(\Delta H_v - \int_{M_i}^{M_f} q_{st}(M) dM \right) \quad (9)$$

434 Here q_{st} is expressed as in Eq. (6) and MW is the molecular weight of water.

435 4.3. XRD

436 XRD provides information on sample structure by measuring the intensity and scattering angle of X-
 437 rays incident on the sample. It was performed in this study to assess changes in carbohydrate structure
 438 following processing. Performing XRD on apples, muntries, and finger limes produced the
 439 diffractograms in Figure 3. Freeze-dried (not frozen) samples are used as a benchmark in these XRD
 440 results to compare with oven-dried samples. Freeze-drying introduces minimal physicochemical
 441 changes compared to oven-drying, and low-moisture samples were required with this instrument
 442 setup. All three XRD diffractograms have broadly consistent diffuse peak contributions reaching
 443 maxima at 21.4° and 37.6°. The major exceptions to this are the sharp peaks at 21.5° and 23.8° in
 444 muntries. The areas under the curves were lower in the oven-dried samples compared to the freeze-
 445 dried: 8.9% lower for apple, 15.3% for muntrie, and 9.8% for finger lime. The diffuse peaks indicate the
 446 predominance of an amorphous structure. Possible origins for the diffuse signals at 21.5° and 23.8°
 447 are the starch and pectin components of the fruits respectively (Mutungi et al., 2012, Kazemi et al.,
 448 2023). The sharp signals in muntries are consistent with the presence of crystalline cellulose (Bezerra
 449 et al., 2014). Assuming structure at this scale is the same in the freeze-dried as in the frozen material,
 450 XRD reveals that oven-drying reduces the integrated intensity of the amorphous signal. This signal loss
 451 suggests that oven-drying reduced the amount of the complex polysaccharides present that
 452 contributed to the diffuse peaks, especially in muntries and finger limes (Appendix 5). This is consistent
 453 with how XRD diffractograms of amorphous gelatinised starch have been reported to have a reduced
 454 amorphous signal following hydrolysis (O'Brien and Wang, 2008) as well as following drying (Ye and
 455 Baik, 2024). It is suggested the processing-induced changes observed in carbohydrate chemistry and
 456 structure are correlated to the changes observed in water sorption (see Section 4.7).



457

458

Figure 3: XRD diffractograms of freeze- and oven-dried (at 60°C): (a) apple; (b) muntrie; (c) finger lime.

459

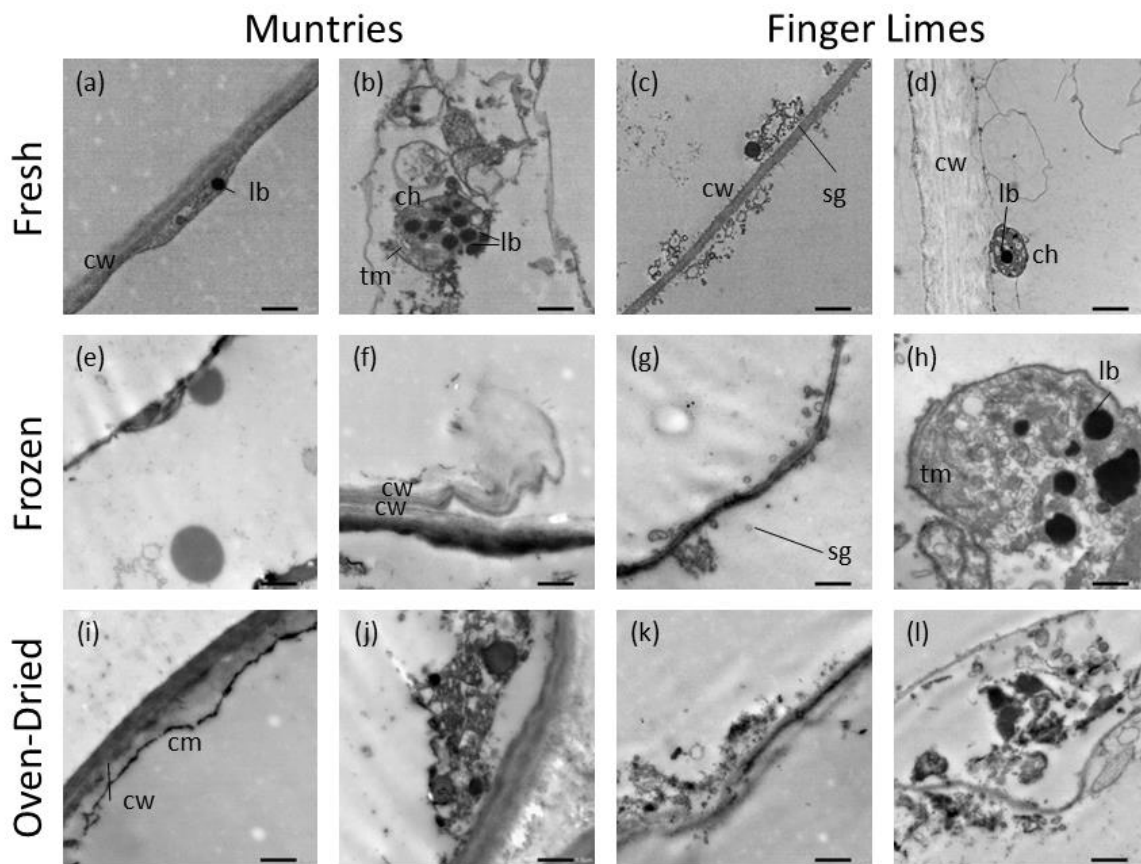
4.4. TEM

460

TEM can be used to image the micro- and nanostructure of a food material and indicate the changes induced by processing. In this work, TEM was used to image the cellular features of apples, muntries, and finger limes when fresh, frozen, and oven-dried (Figure 4). Representative TEM images were selected for Figure 4, with select annotations describing proposed ultrastructural features. Chloroplasts undergoing degradation of their thylakoid membranes into lipid bodies can be observed in the fresh finger limes and muntries (Figure 4 (b, d)). Starch crystals are tentatively identified as associated with the cell wall of a parenchymal cell in fresh finger lime (Figure 4 (c, g, k)). Finger limes (in Figure 4 (c, d, g, h, k, l)) as an example of a hesperidium, contain juice vesicles (the edible portion of the fruit) that are multicellular sacs. The structures identified in the finger limes are similar to those that have been identified in fully ripe juice vesicles of grapefruit, another hesperidium (Burns et al., 1992). The chloroplasts can also be observed breaking up and being exposed by the freezing and especially the drying process in both the muntries and the finger limes (Figure 4 (b, j, d, h, l)). As the muntries were first frozen (Figure 4 (e, f)) and then dried (Figure 4 (i)), the cell membrane deformed

472

473 and separated as the cell wall loosened. This is similar to what has been observed occurring during
 474 ripening of Goji berry, where berry mesocarp was also studied (Zhang et al., 2024). In studying Goji
 475 berry ripening, Zhang et al. (2024) linked this phenomenon to the depolymerisation of cell wall
 476 polysaccharides by enzymes associated with ripening. The micrographs indicate processing-induced
 477 changes to the fruit cellular features consistent with the opening up of these features and the
 478 depolymerisation of their carbohydrate components. The correlation of this to changes in water
 479 binding are further discussed in Section 4.7.



480

481 *Figure 4: TEM micrographs of fresh, frozen, and oven-dried (at 60°C) muntries and finger limes. Scale bar represents 1.0 μm.*

482 *cw - cell wall; sg - starch granules; cm – cell membrane; ch - chloroplast; tm – thylakoid membrane; lb – lipid bodies.*

483 4.5. Macronutritional Content

484 Characterising the macronutrient composition of ANFs is necessary for understanding their nutritional
 485 and health applications but can also give insight into their physicochemical properties. The
 486 carbohydrate and energy content of apples and muntries were similar, varying from 15-18 g/100 g w.b.

487 and 238-299 kJ/100 g respectively, with muntries having the greater carbohydrate content and
 488 therefore energy content. Finger limes were not as rich in carbohydrates or energy, however, with 13
 489 g/100 g w.b. and 177 kJ/100 g respectively. On a dry basis the fruits were all between 87.1 and 97.5%
 490 carbohydrate. Of the macronutrients, statistical testing was conducted on the protein contents. One-
 491 way ANOVA and Tukey tests demonstrated the protein contents of the ANFs (0.99 g/100 g w.b. for
 492 muntries and 0.83 g/100 g for finger limes) were significantly ($p < 0.05$) greater than for apple (0.13
 493 g/100 g). Apples and finger limes were measured as having similar moisture contents (84.1 and 84.2
 494 g/100 g w.b. respectively) while muntries were relatively low in moisture (79.7 g/100 g). The ANFs
 495 were measured as being higher in fat than apple (0.27 - 0.63 g/100 g vs. 0.08 g/100 g) as well as higher
 496 in ash (0.79 - 0.57 g/100 g vs. 0.19 g/100 g). The macronutrient contents measured for apples are
 497 broadly consistent with reference values from the USDA (see Table 1).

498 *Table 3: Macronutritional profiles of apple, muntrie, and finger lime (per 100 g w.b.). Values attached to different letters are*
 499 *statistically significant to each other ($p < 0.05$).*

	Apple	Muntrie	Finger Lime
Moisture (g)	84.14 ± 1.91	79.70 ± 1.73	84.23 ± 3.58
Protein (g)	0.1267 ± 0.0101 ^a	0.9946 ± 0.0389 ^b	0.8272 ± 0.1784 ^b
Fat (g)	0.078 ± 0.10	0.27 ± 0.07	0.63 ± 0.52
Ash (g)	0.1934 ± 0.0079	0.7859 ± 0.0201	0.5739 ± 0.0374
Carbohydrate (g)	15.46 ± 0.37	18.24 ± 0.40	13.74 ± 0.80
Energy (kJ)	238.0 ± 0.4	299.0 ± 0.4	176.6 ± 1.0

500 4.6. Sugar Contents

501 Because of their prevalence in fruit, their nutritional relevance, and the strong influence of sugars on
 502 water-binding in food (Rao et al., 2005), fructose, glucose, and sucrose were also measured via
 503 enzymatic assay (Table 4). Two-way ANOVA was used to assess statistical significance of samples
 504 measured in triplicate. Among the undried (frozen) fruit, sucrose, glucose, and fructose were all
 505 highest in apple. Glucose and fructose were significantly ($p < 0.05$) greater in apple than in muntrie,
 506 itself significantly greater than in finger lime. Sucrose was also significantly greater in apple than in
 507 muntrie. Since muntries contained more total carbohydrates than apple while apple contained more
 508 of the sugars measured, it is suggested complex carbohydrates comprise a greater portion of the
 509 carbohydrate content in muntries than in apples. The measured contents of glucose, sucrose, and
 510 fructose in apple changed from 10.5%, 28.8%, and 43.3% to 11.3%, 32.1%, and 50.3 % respectively
 511 after drying. At the same time, the increase in glucose and fructose content in muntries was from
 512 10.4% to 15.4% and from 16.6% to 22.6% respectively, while sucrose decreased from 17.5% to 10.8%.

513 Finger limes, too, saw an increase in glucose (1.6% to 2.6%) as well as an increase in fructose (2.4% to
 514 5.0%). Sucrose was not detected in finger limes within the detection limit of the assay. Relative to the
 515 initial frozen values, drying had less effect on the glucose, sucrose, and fructose contents of apple
 516 compared to the ANFs. The changes to the concentrations of sucrose and fructose in all fruit
 517 considered following drying were not substantial enough to be statistically significant. However, drying
 518 caused a statistically significant ($p < 0.05$) increase in the glucose content of all fruits. In addition, the
 519 effect of drying on glucose content was significantly ($p < 0.05$) greater for both muntries and for finger
 520 limes compared to apples. Macronutritional and sugar contents indicate consistency with the
 521 previously reported upon tendency for ANFs to be relatively protein-rich compared to conventional
 522 fruits, as well as containing lower sugar contents even when higher in carbohydrates overall (Richmond
 523 et al., 2019).

524 *Table 4: Changes in sugar contents as a result of oven-drying (at 60°C) of apple, muntrie, and finger lime (per 100 g d.b.).*
 525 *Values attached to different superscripts are statistically significant to each other ($p < 0.05$).*

	Apple		Muntrie		Finger Lime	
	Frozen	Dried	Frozen	Dried	Frozen	Dried
Glucose	10.5 ± 1.9 ^{a1}	11.3 ± 2.3 ^{a2}	10.4 ± 1.0 ^{b3}	15.4 ± 0.1 ^{b4}	1.6 ± 0.4 ^{c5}	2.6 ± 0.2 ^{c6}
Sucrose	28.8 ± 8.7 ^d	32.1 ± 3.5 ^d	17.5 ± 1.0 ^e	10.8 ± 2.7 ^e	ND	ND
Fructose	43.3 ± 9.9 ^f	50.3 ± 8.1 ^f	16.6 ± 1.8 ^g	22.6 ± 1.0 ^g	2.4 ± 0.9 ^h	5.0 ± 2.2 ^h

526 **4.7. Comparison of Changes in Sorption to Changes in Carbohydrates**

527 As demonstrated in Section 4.1, the moisture sorption isotherms for ANFs showed the binding of water
 528 to the fruit matrix (at temperatures of 40°C and 60°C) was increased after drying. This was contrary to
 529 the sorption behaviour of other similar foods, including apples. The extent of this effect depended on
 530 drying temperature and drying methods. The processing method that produced the largest effect
 531 depended on whether the isotherm was examined above or below an a_w of 0.6-0.8. In simple systems
 532 with minimal physical or chemical changes, increases in temperature have the general effect of
 533 decreasing sorption due to reduced entropy differences between the adsorbate and unadsorbed
 534 material. However, it is not uncommon for food systems to contradict this trend due to physical or
 535 chemical temperature-induced material changes (Rao et al., 2005). In particular, the changes in sugar
 536 solubility at high water activities (~ 0.8) is known to cause significant deviation. The water activity range
 537 above which sugar solubility and crystallinity have significant effects on sugar-rich foods in literature is
 538 the same water activity at which the effect of processing on ANF isotherms changed. It is therefore
 539 suggested that the uncharacteristic sorption phenomena observed in ANFs are due to drying-induced
 540 changes to the sugars present.

541 The changes to the sugar profiles, the cellular features, and the XRD diffractograms that occur as a
542 result of drying support this hypothesis. All samples displaying a reduced amorphous signal after drying
543 suggests the conversion of some portion of the complex carbohydrates present to simpler
544 carbohydrates. Drying was also correlated with the breaking up of organelles and increased area of
545 exposure. Simultaneously, while sucrose and fructose contents are not significantly affected by drying
546 (suggesting inversion is not an explanation), glucose contents are increased significantly, especially in
547 the ANFs. A mechanism for this may be that, during early stages of the drying process when water
548 activity is still high enough for unhindered enzymatic activity, the elevated temperatures of drying
549 allow amylases/glucosidases to convert part of the fruits' starch reserves to glucose. Isomerases may
550 then further partially convert this to fructose. ANFs may see a greater relative increase in these
551 monosaccharides because of a greater activity of these enzymes. This is supported by the fact that the
552 greatest relative increase in fructose and glucose as a result of drying occurred in muntries, suggested
553 by the combination of their macronutritional and sugar profiles to be richer in more complex
554 carbohydrates. It is proposed that this may be a protective mechanism that ANFs have evolved to allow
555 survival in droughts by more substantial access to stored carbohydrate energy in low-moisture
556 circumstances.

557 This effect of drying on carbohydrate chemistry is also reflected in the decrease in monolayer enthalpy
558 as obtained by the fitting of the net isosteric heat of sorption equation (Eq. (6)). The free
559 monosaccharides, with their exposed hydroxyl groups, would present more active sites onto which
560 water can bind, with this solvation layer also being more energetically favourable. Besides supporting
561 the hypothesis described above, the heat of sorption model suggested in this work has the benefit of
562 being a novel and analytical approach to describing sorption phenomena in food systems. Its validity
563 is reinforced by the close agreement with the data reported here. An example of an engineering
564 application is given in Appendix 4. Here the heat required to dry 1 kg each of apples and muntries to
565 a water activity of 0.4 is calculated to be 49 and 92 kJ respectively, reflecting the increased binding
566 energy in muntries. It is proposed that this may be a valuable tool in the design of food dryers for
567 minimal processing by providing the ability to predict energy requirements that can be tuned
568 according to product specifications.

569 5. Conclusions

570 ANFs are crops of significant interest due to their drought tolerance but which lack the characterisation
571 required for larger-scale processing and use, especially when it comes to how they can be most
572 optimally preserved. An understanding of the processing-property relationships and the effects of

573 processing on shelf-stability of any fruit requires a better understanding of how processing affects the
574 behaviour of the water they contain. This has been addressed in this work by the quantification of
575 water sorption isotherms for finger limes and muntries and subsequent determination of the GAB
576 model as the most suitable descriptor of how they bind moisture. The effects of temperature and
577 processing on these sorption phenomena were measured, showing the unique phenomenon of an
578 increased ability to bind water in muntries and finger limes following drying. XRD and TEM revealed
579 an opening up of cellular features and a reduction in the amount of amorphous complex carbohydrates
580 during drying. Macronutritional and sugar characterisation demonstrated high protein contents as well
581 as a significant drying-induced increase in glucose content. The increase in water binding after drying
582 in ANFs is suggested to be the result of more substantial hydrolysis of complex polysaccharides during
583 drying. The temperature variation of the isotherms was also used to determine the net isosteric heat
584 of sorption as a function of moisture content, with a precision that allowed the derivation of a novel
585 analytical expression for this function. Applications of this expression include the calculation of the
586 heat required to dry the fruits studied to a target water activity. These results provide tools for the
587 engineering of drying processes to extend ANF shelf-life as much as needed while drying as little as
588 possible for the water activity needed. This allows for reduced energy use in drying and minimal quality
589 losses. The models and techniques developed in this paper allow this not only for ANFs but for the
590 more sustainable processing of foods more generally.

591 Acknowledgments

592 The authors wish to acknowledge the traditional custodians of the land where the work of this project
593 took place, the Bunurong people of the Kulin Nation, as well as the traditional custodians of the
594 Wotjobaluk, Jaadwa, Jadawadjali, Wergaia and Jupagulk people on whose lands the foods that were
595 studied were grown. The authors wish to pay respects to their Elders, past and present and to their
596 continual connection to the lands.

597 The authors especially wish to thank the traditional growers who shared their knowledge to aid this
598 project, in particular Elizabeth Mace a Wotjobaluk, Jadawadjali and Wergaia Woman from the Barengi
599 Gadjin Land Council.

600 Special thanks also go to Ni Ni Well and OZ Finger Lime for their insights and samples.

601 Declaration of interest statement

602 The authors declare that they have no known competing financial interests or personal relationships
603 that could have appeared to influence the work reported in this paper.

604 References

- 605 AL-MUHTASEB, A. H., MCMINN, W. A. M. & MAGEE, T. R. A. 2002. Moisture Sorption Isotherm
606 Characteristics of Food Products: A Review. *Food and Bioproducts Processing*, 80, 118-128.
- 607 AOAC, J. 2005. *Official Methods of Analysis of AOAC International*, Gaithersburg, MD, USA.
- 608 BEN HAJ SAID, L., BELLAGHA, S. & ALLAF, K. 2015. Measurements of texture, sorption isotherms and
609 drying/rehydration kinetics of dehydrofrozen-textured apple. *Journal of Food Engineering*, 165,
610 22-33.
- 611 BEZERRA, R., SILVA, M., MORAIS, I., OSAJIMA, J., SANTOS, M., AIROLDI, C. & FILHO, E. 2014. Phosphated
612 Cellulose as an Efficient Biomaterial for Aqueous Drug Ranitidine Removal. *Materials*, 7, 7907-
613 7924.
- 614 BURNS, J., ACHOR, D. & ECHEVERRIA, E. 1992. Ultrastructural Studies on the Ontogeny of Grapefruit
615 Juice Vesicles (*Citrus paradisi* Macf. CV Star Ruby). *International Journal of Plant Sciences - INT J*
616 *PLANT SCI*, 153.
- 617 CHUNG, D. S. & PFOST, H. B. 1967. Adsorption and Desorption of Water Vapor by Cereal Grains and Their
618 Products Part I: Heat and Free Energy Changes of Adsorption and Desorption. *Transactions of*
619 *the ASABE*, 10, 549-0551.
- 620 ESCOBEDO-AVELLANEDA, Z., VELAZQUEZ, G., TORRES, J. A. & WELTI-CHANES, J. 2012. Inclusion of the
621 variability of model parameters on shelf-life estimations for low and intermediate moisture
622 vegetables. *LWT*, 47, 364-370.
- 623 FRANCINI, A. & SEBASTIANI, L. 2013. Phenolic Compounds in Apple (*Malus x domestica* Borkh.):
624 Compounds Characterization and Stability during Postharvest and after Processing.
- 625 GLOVER, R., TAYLOR, T., REDMAN, M. & TRAINER, P. 2021. Australian Native Finger Lime RD&E Plan.
626 AgriFutures.
- 627 HOSSAIN, M. D., BALA, B. K., HOSSAIN, M. A. & MONDOL, M. R. A. 2001. Sorption isotherms and heat
628 of sorption of pineapple. *Journal of Food Engineering*, 48, 103-107.

629 IGLESIAS, H. A. & CHIRIFE, J. 1978. An Empirical Equation for Fitting Water Sorption Isotherms of Fruits
630 and Related Products. *Canadian Institute of Food Science and Technology Journal*, 11, 12-15.

631 JEANTET, R. 2016. *Handbook of food science and technology. 1, Food alteration and food quality*, London
632 : Hoboken, London : ISTE, Ltd. Hoboken : Wiley.

633 KAYMAK-ERTEKIN, F. & GEDIK, A. 2004. Sorption isotherms and isosteric heat of sorption for grapes,
634 apricots, apples and potatoes. *Food science & technology*, 37, 429-438.

635 KAZEMI, M., ABOUTALEBZADEH, S., MOJAVERIAN, S. P., SAMANI, S. A., KOUHSARI, F., POURVATANDOUST,
636 S., SALIMI, A., SAVAROLYIA, M., NAJAFI, A., HOSSEINI, S. S. & KHODAIYAN, F. 2023. Valorization
637 of pistachio industrial waste: Simultaneous recovery of pectin and phenolics, and their
638 application in low-phenylalanine cookies for phenylketonuria. *International Journal of Biological
639 Macromolecules*, 249, 126086.

640 KIRANOUDIS, C. T., MAROULIS, Z. B., TSAMI, E. & MARINOS-KOURIS, D. 1993. Equilibrium moisture
641 content and heat of desorption of some vegetables. *Journal of Food Engineering*, 20, 55-74.

642 LAURIE, S. 2020. Australian native foods and botanicals- 2019/20 market study. ANFAB.

643 MAROULIS, Z. B., TSAMI, E., MARINOS-KOURIS, D. & SARAVACOS, G. D. 1988. Application of the GAB
644 model to the moisture sorption isotherms for dried fruits. *Journal of food engineering*, 7, 63-
645 78.

646 MERRILL, A. L. 1973. Energy Value of Foods: Basis and Derivation. *In: AGRICULTURE*, U. S. D. O. (ed.).

647 MORAGA, G., MARTÍNEZ-NAVARRETE, N. & CHIRALT, A. 2006. Water sorption isotherms and phase
648 transitions in kiwifruit. *Journal of Food Engineering*, 72, 147-156.

649 MORAGA, G., TALENS, P., MORAGA, M. J. & MARTÍNEZ-NAVARRETE, N. 2011. Implication of water
650 activity and glass transition on the mechanical and optical properties of freeze-dried apple and
651 banana slices. *Journal of Food Engineering*, 106, 212-219.

652 MOREIRA, R., CHENLO, F., TORRES, M. D. & VALLEJO, N. 2008. Thermodynamic analysis of experimental
653 sorption isotherms of loquat and quince fruits. *Journal of Food Engineering*, 88, 514-521.

654 MUTUNGI, C., PASSAUER, L., ONYANGO, C., JAROS, D. & ROHM, H. 2012. Debranched cassava starch
655 crystallinity determination by Raman spectroscopy: Correlation of features in Raman spectra
656 with X-ray diffraction and ¹³C CP/MAS NMR spectroscopy. *Carbohydrate Polymers*, 87, 598-606.

657 NETZEL, M., NETZEL, G., TIAN, Q., SCHWARTZ, S. & KONCZAK, I. 2007. Native Australian fruits — a novel
658 source of antioxidants for food. *Innovative Food Science & Emerging Technologies*, 8, 339-346.

659 O'BRIEN, S. & WANG, Y.-J. 2008. Susceptibility of annealed starches to hydrolysis by α -amylase and
660 glucoamylase. *Carbohydrate Polymers*, 72, 597-607.

661 ORIAN, G. H. & MILEWSKI, A. V. 2007. Ecology of Australia: the effects of nutrient-poor soils and intense
662 fires.

663 RAO, M. A., RIZVI, S. S. H. & DATTA, A. K. 2005. *Engineering properties of foods*, Boca Raton, Taylor &
664 Francis.

665 RICHMOND, R., BOWYER, M. & VUONG, Q. 2019. Australian native fruits: Potential uses as functional
666 food ingredients. *Journal of Functional Foods*, 62, 103547.

667 SALO-VÄÄNÄNEN, P. P. & KOIVISTOINEN, P. E. 1996. Determination of protein in foods: comparison of
668 net protein and crude protein ($N \times 6.25$) values. *Food Chemistry*, 57, 27-31.

669 SENEVIRATNE, S. I., ZHANG, X., ADNAN, M. & W. BADI; C. DERECZYNSKI, A. D. L., S. GHOSH, I. ISKANDAR,
670 J. KOSSIN, S., LEWIS, F. OTTO, I. PINTO, M. SATOH, S.M. VICENTE-SERRANO, M. WEHNER, B.
671 ZHOU 2023. Weather and Climate Extreme Events in a Changing Climate. *In:*
672 INTERGOVERNMENTAL PANEL ON CLIMATE, C. (ed.) *Climate Change 2021 – The Physical Science*
673 *Basis: Working Group I Contribution to the Sixth Assessment Report of the Intergovernmental*
674 *Panel on Climate Change*. Cambridge: Cambridge University Press.

675 TSAMI, E. 1991. Net isosteric heat of sorption in dried fruits. *Journal of Food Engineering*, 14, 327-335.

676 TSAMI, E., KROKIDA, M. K. & DROUZAS, A. E. 1998. Effect of drying method on the sorption
677 characteristics of model fruit powders. *Journal of Food Engineering*, 38, 381-392.

678 TSAMI, E., MAROULIS, Z. B., MARINOS-KOURIS, D. & SARAVACOS, G. D. 1990. Heat of sorption of water
679 in dried fruits. *International Journal of Food Science & Technology*, 25, 350-359.

680 USDA 2018. Apples, raw, with skin (Includes foods for USDA's Food Distribution Program).

681 VAN 'T HAG, L., DANTHE, J., HANDSCHIN, S., MUTULI, G., MBUGE, D. & MEZZENGA, R. 2020. Drying of
682 African Leafy Vegetables for Their Effective Preservation: Difference in Moisture Sorption
683 Isotherms Explained by their Microstructure. *Food & Function*, 11.

684 YE, S.-J. & BAIK, M.-Y. 2024. Physicochemical properties of amorphous granular starch (AGS) prepared
685 by non-thermal gelatinization by high hydrostatic pressure (HHP) and spray drying. *International*
686 *Journal of Biological Macromolecules*, 260, 129508.

687 ZHANG, A.-A., XIE, L., WANG, Q.-H., XU, M.-Q., PAN, Y., ZHENG, Z.-A., LV, W.-Q. & XIAO, H.-W. 2024. Effect
688 of the ripening stage on the pulsed vacuum drying behavior of goji berry (*Lycium barbarum* L.):
689 Ultrastructure, drying characteristics, and browning mechanism. *Food Chemistry*, 442, 138489.